Landslides (2005) 00
DOI: 10.1007/s10346-005-0001-4
Received: 31 December 2004
Accepted: 14 June 2005

Ashok K. Chugh · Timothy D. Stark

Permanent seismic deformation analysis of a landslide

Abstract A failed slope may not necessarily require a remedial treatment if it can be shown with confidence that the maximum movement of the slide mass will be within tolerable limits, i.e., not cause loss of life or property. A permanent displacement analysis of a landslide for static and seismic conditions is presented using a continuum mechanics approach. Computed values of displacement for static conditions compare favorably with field measurements and computed values of seismic displacements for a postulated earthquake motion appear reasonable. Also, the seismic displacements using the continuum mechanics approach compare favorably with those obtained using the Newmark sliding block procedure for assessing seismically-induced slope deformations.

Keywords Landslide · Slope failure · Displacement · Continuum mechanics · Analysis

Introduction

After some movement, the slide mass of a landslide will come to rest in a more stable configuration. The amount of movement is a function of the failure mechanism. The cause of the landslide may be static, such as build-up of pore-water pressures in the soil mass, steepening of slope, toe excavation, an increase in surface loads, etc., or dynamic, such as an earthquake, blasting, traffic-induced vibrations, etc. Environmental factors such as desiccation cracking followed by ingress of surface water from a rain storm can also trigger landslides. Whatever the cause of a landslide (initial failure), the failed mass comes to rest in a more stable configuration. Sometimes, the newly acquired stable configuration can be reactivated under a new or different set of surface and/or subsurface conditions.

Generally, one is interested in analyzing a slope for the onset of failure whether it is for the first-time occurrence or a reactivation of a slide using appropriate material properties, and surface and subsurface conditions. In such cases, the results of analyses are used to design/implement measures to assure stability of the slope for the desired conditions. There are several numerical analysis procedures available to calculate the factor of safety (FoS) for the before- and after- the failure conditions at a site. These methods differ in complexity, data needs, and accuracy of results—but their primary objective is to calculate the FoS against failure. These numerical-analysis procedures are based on either limit-equilibrium or continuum-mechanics theories.

In some situations, the onset of a slope failure is not of primary concern if the slide mass will not encroach on another piece of property, endanger life, or otherwise have a material effect on the environmental/other interests of a site. In this situation, the primary concern is the magnitude of displacement of the slide mass. This is the problem of interest in the study reported in this paper.

Motivation

During the design phase of an embankment dam, 32 different historic landslides were mapped and analyzed in the field within the reservoir area and adjacent hills (Fig. 1). A summary description of these 32 slides is given in Chugh and Stark 2005. In addition to these 32 numbered landslides, there are 17 landslides that are identified but not numbered or described. It was anticipated in the design phase (1980s) that areas within the reservoir containing fat-clay topsoils, overlying predominantly fine-grained soil units with north- to northwest facing slopes of 2H:1V (2 horizontal to 1 vertical) to 5.5H:1V that had failed in the past would be susceptible to additional sliding due to likely seepage of reservoir water into the pervious sand units. With the filling of the reservoir, this prediction came true with about 20 slides occurring. Fig. 1 conveys the complexity of the geologic environment and the enormity of the landslide activity in this relatively small area. The geologic units at the site are composed of unindurated, compacted sediments deposited in both marine and lacustrine environments. The geologic units are estimated to be over 2500 m thick consisting of interbedded lean and fat clays and silty and clayey sands. These deposits are overlain by an average of 1 m thick fat-clay.

At present, the area of most of the landslides is remote and does not merit extensive analyses or remedial measures. However, the toe of one of the the landslides, identified as Quaternary landslide

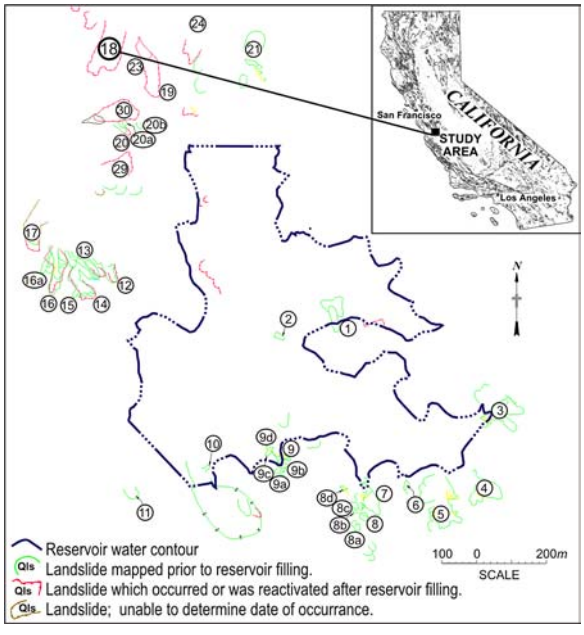

Fig. 1 Location map of landslide study area

(Qls)-18 in Fig. 1, is within about 50 m of a developed facility. This close proximity of Qls-18 to development motivated this study to determine if landslide Qls-18 could reach the development before or after a seismic event?

Objectives

The objectives of this paper are to present

1. An effective and efficient procedure to estimate the post-failure maximum displacement of a slide mass due to static and seismic conditions; and
2. An application of the procedure to the Qls-18 landslide shown in Fig. 1.

The proposed procedure can be implemented in essentially any continuum-mechanics based solution procedure; however, for analysis of the field problem presented in this paper, a commercially available computer program FLAC (Itasca Consulting Group 2000) was used. FLAC is an acronym for Fast Lagrangian Analysis of Continua; it is a two-dimensional explicit finite difference program; and its adoption was for convenience.

For static analyses, computed displacements are compared with the field measurements; and for dynamic analyses, the computed displacements are compared with those obtained using the Newmark sliding block procedure for estimating seismically-induced slope deformations (Newmark 1965). The Newmark procedure is implemented in the computer program DISP (Chugh 1980). Relative merits of using FLAC and DISP for assessing the earthquake-induced displacements are mentioned. Copies of the computer program DISP and instructions for its use can be obtained from the first author on request.

Rationale

The rationale for the proposed procedure is the following:

(a) If a landslide has occurred previously, there is little to be gained by performing slope stability analyses, especially when the field conditions that caused the slope failure and the location of the slip surface have been well estimated/determined via field work and material properties are well established via laboratory/field tests.

(b) If a slope has not failed, FoS results from slope stability analyses can be used to reduce the values of shear strength parameters (cohesion and friction angle) to bring the soil mass to the verge of failure, i.e., static FoS = 1.
Steps (a) and (b) mark the beginning of displacement of the slide mass.

(c) An estimate of horizontal and vertical displacements of a soil mass above the potential failure surface, items (a) and (b), due to a static cause can be made via a continuum-mechanics based solution procedure. At the end of this step, the slide mass would have come to rest in a stable geometric configuration. This stable geometric configuration of the slide mass may be permanent or temporary depending on status quo of the event(s) that initiated the slope failure or occurrence of a new destabilizing event (such as an earthquake), respectively.

(d) An estimate of horizontal and vertical displacement of the slide mass above the potential failure surface caused by a seismic event can also be made via a continuum-mechanics based solution procedure.

(a) March 2004 photographic view.

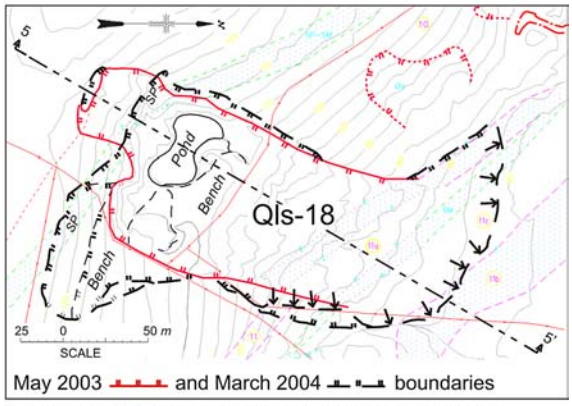

(b) Plan view of the May 2003 and March 2004 boundaries.

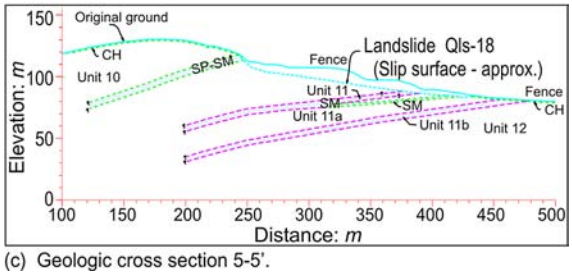

(c) Geologic cross section 5-5'.

Fig. 2 Descriptions of the Qls-18 landslide

(e) The Newmark sliding block procedure for calculating permanent deformations of a slide mass due to earthquake loading is an efficient alternative to the continuum approach, item (d).

Proposed continuum-mechanics based procedure

The proposed procedure for calculating permanent displacement of a slide mass for static and seismic conditions using the continuum-mechanics approach has the following steps:

(a) Create a discretized model of the continuum considering its use for static and dynamic analyses and identify the locations where displacement results are of interest;

(b) Include in step (a), the failure surface of interest as an interface between the soil mass above the failure surface and the intact soil mass below the failure surface;

(c) Assign appropriate material properties to the continuum materials and the interface. Apply the appropriate surficial loads and boundary conditions to the numerical model for static analysis;

(d) Perform a static deformation analysis using a large displacement and large strain formulation (updated Lagrangian and large strain constitutive formulation). At the end of this analysis, the model should be in equilibrium.
(e) If necessary, change material/interface properties to reflect the field conditions, and repeat step (d).
This is the end of static deformation analysis and the calibrated parameters will be used for the seismic analysis. Additional details on the static analysis are given in Chugh and Stark (2005). To continue with the dynamic deformation analysis using the continuum approach, the proposed procedure has the following steps:
(f) To the last execution of step (d), apply the appropriate dynamic boundary conditions, shear strength parameters, and seismic time-acceleration history to the model;
(g) Perform the deformation analysis for the dynamic conditions using a large displacement and large strain formulation (similar to step (d)) for the duration of the seismic event;
(h) At the end of the seismic event, continue the analysis for free vibrations for a reasonable length of time to study the post-seismic response of the model.

Newmark sliding block procedure

As an alternative to the continuum approach for dynamic deformation analysis (steps (f), (g), and (h) under the heading 'Proposed continuum-mechanies based procedure'), the Newmark sliding block analysis (Newmark 1965) can be used to calculate permanent displacements of the slide mass due to an earthquake. The Newmark procedure is an efficient alternative to the continuum approach. However, confidence in an exclusive use of one of the two alternatives needs further study (analysis of landslides/slope-failures); in the interim, both methods should be used for comparison of results and to gain confidence in the final outcome of the analyses.

Sample problem

The chronology of the landslides in the area around the reservoir indicates that the Qls-18 landslide occurred or was reactivated subsequent to the first filling of the reservoir. Seepage from the reservoir entering the underlying pervious sand units has been attributed to be the cause of the Qls-18 and other landslides west and northwest of the reservoir (U.S. Bureau of Reclamation 2004). The Qls-18 landslide is about 10 m thick and occurred in a 4.5H:1V ground slope on the hillside facing away from the reservoir; and the slide materials include fat-clay topsoil and underlying Quaternary Pliocene-Pleistocene sediments (QPs) of the marine and lacustrine environments.

In May 2003, new Qls-18 landslide movement began to occur in the area immediately adjacent to, and to the east of, the head scarp of the historic limits of the Qls-18 landslide. Water levels in an observation well (located in the lower portion of the slope and just to the east of the historic limits of the Qls-18 landslide) had risen by about 9 m above historic levels. Seepage exiting the Qls-18 landslide area had increased from an average of 10– 15 liters per minute (L/min) to about 400 L/min. At this time, very limited downslope movement and only minor ground distortion immediately downslope of the new (1–2.5 m high and about 60 m across at the top) head scarp had occurred.

By March 2004, the 2003 head scarp had developed into a new lobe of sliding, about 60 m wide, that along with portions of the 2003 slide had moved 23–30 m downslope in the toe area; and the head scarp in the new lobe of sliding was about 7.5–9 m high. Also, the western side-scarp in the old portion of Qls-18 had additional movement during May 2003 and March 2004. Seepage exiting the Qls-18 landslide area had decreased to 10–15 L/min. Water flowing from the head scarp was ponding on a newly formed bench just downslope from the head scarp—the pond covered an area of about 8000 m^2 and the water depth was about 1–1.5 m. The observation well (that formerly was just east of the limits of the Qls-18 landslide) was in a downslope portion of the new Qls-18 landslide area and was destroyed.

Table 1 summarizes the 2003 and 2004 movement data for the Qls-18 landslide. The distance from the March 2004 toe of the landslide to the nearest building downslope is about 50 m. Descriptions of the Qls-18 landslide in terms of the March 2004 photographic view, the May 2003 and March 2004 boundaries, and the geologic cross section with different soil units in the hillside are shown in Fig. 2a, b, and c, respectively. The location and geometry of the failure surface shown in Fig. 2c were estimated in the field from observations of the scarp and toe of the slide and data from drill logs.

Material properties

Because of the interbedded nature of the QPs, the foundation soils are grouped into the major geologic units shown in Fig. 2c. Soils from different geologic units were tested to determine the fully-softened and residual shear-strengths using triaxial compression, and repeated direct-shear and torsional ring shear tests, respectively. All laboratory tests were performed in the 1980s for the design of the dam and appurtenant structures. Shear and bulk modulus values were assumed. The interface strength properties correspond to those of the slide mass, and the stiffness values were assumed. Table 2 shows the material properties and Table 3 shows the interface (slip surface) properties used in the deformation analyses of the Qls-18 landslide.

Groundwater condition

The water table in the Qls-18 landslide was assumed to be at the top of the SP-SM layer (elevation 120 m) and then followed the field-estimated slip surface shown in Fig. 2c.

Earthquake motion

The Yerba Buena Island record of the 1989 Loma Prieta, California, earthquake (Ms = 7.1 and a_{max} = 0.3 g) was selected for estimating additional movements of the slide mass due to an earthquake event in the near vicinity. Figure 3a shows the time-acceleration data of the earthquake motion used for seismic-deformation analyses of the Qls-18 landslide. Direct integration of the input motion is shown in Fig. 3b; and direct integration of time-velocity data, Fig. 3b, is shown in Fig. 3c. Integeral of complete input motion results in approximately 0.001 m/s velocity and 0.066 m displacement. Thus, the earthquake motion used is essentially free of baseline error. Figure 3d shows the Fourier power spectrum of the input motion.

Numerical analyses

For numerical analyses of the landslide conditions of May 2003 (assuming first time occurrence due to high ground-water condi-

Table 1 Field data on Qls-18 landslide movements

May 2003		March 2004	
Downslope movement at new head scarp (m)	Vertical drop at new head scarp (m)	Downslope movement at toe of Qls-18 (m)	Vertical drop at new head scarp (m)
Very limited	1–2.5	23–30	7.5–9

Table 2 Material properties for stability and deformation assessments of Qls-18 landslide

Material identifier	Density ρ(kg/m^3)	Material strength		Elastic constants	
		c′ (kPa)	φ′ (°)	Bulk modulus 10^7 (kPa)	Shear modulus 10^7 (kPa)
CH	1970	14	16	1.5	1.0
Unit 10	1970	14*	12*	1.5	1.0
SP-SM	2000	0	35	1.5	1.0
Unit 11	2000	0	35	1.5	1.0
Unit 11a	1800	14	12	1.5	1.0
Unit 11b	1800	0	27	1.5	1.0
SM	1940	0	27	1.5	1.0
Unit 12	1970	14*	12*	1.5	1.0

*Residual shear strength values: c=o, $\varphi' = 6^\circ$

Materials are assigned tensile strength = c/tan φ

Table 3 Interface properties for FLAC model analyses of Qls-18 landslide

Condition	Interface properties			
	c (kPa)	φ (°)	Normal stiffness 10^5 (kPa/m)	Shear stiffness 10^3 (kPa/m)
May 2003	14	16	2	6
March 2004	0	6	2	6
Seismic (future)	0	6	2	6

tions and limited movements), fully-softened shear strengths and other material properties shown in Table 2, interface properties corresponding to the fully-softened shear strengths shown in Table 3, and the water table at top of the SP-SM layer (elevation 120 m) and flowing along the field-estimated slip surface are used.

For numerical analyses of the landslide conditions of March 2004 (substantial movements, observed water pond, normal seepage-flow conditions), fully-softened shear strengths and other material properties shown in Table 2, interface properties corresponding to the residual shear strengths shown in Table 3, and water table at

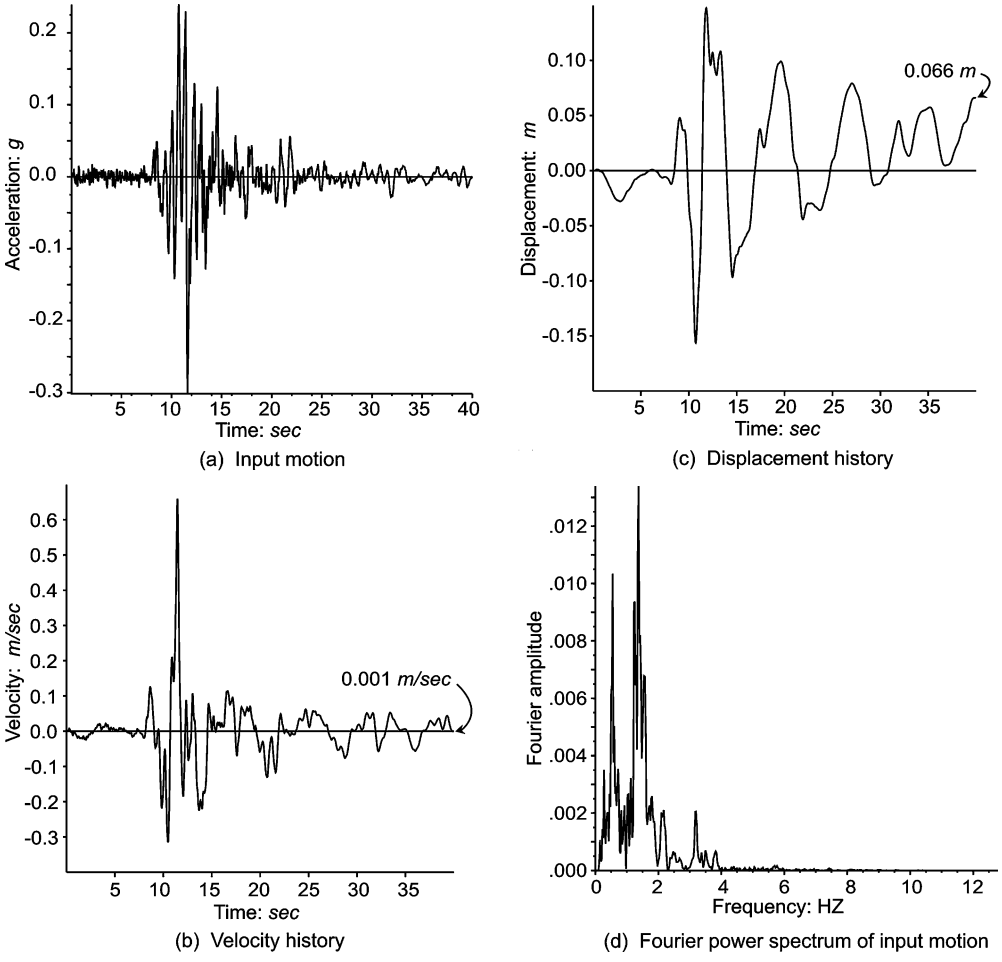

Fig. 3 Loma Prieta earthquake motion. **a** Acceleration time-history. **b** Direct integration of time-history (a). **c** Direct integration of time-history (b). **d** Fourier power spectrum of time- history (a)

top of the SP-SM layer (elevation 120 m) and flowing along the field-estimated slip surface are used.

For analysis of the expected movements during an earthquake, the numerical model at the end of the March 2004 landslide and the associated material and interface properties are used.

FLAC model

Figure 4 is a numerical model of the geologic cross section of the Qls-18 landslide shown in Fig. 2c, and was used in all continuum-based FLAC analyses. The estimated slip surface is modeled as a frictional interface between the slide mass and the parent material (base). Along this interface, the slide mass was allowed to: (a) move relative to the base; and (b) separate from the base. The interface properties are shown in Table 3. The continuum material properties are presented in Table 2; and the water table is shown in Fig. 4. The boundary conditions for static analysis are shown in Fig. 4a, and the boundary conditions for seismic analysis are shown in Fig. 4b. The constitutive model used is Mohr-Coulomb. The displacements of the slide mass were sampled at three locations shown in Fig. 4a.

Static displacements

Deformation analysis of the model in Fig. 4a was started with the May 2003 conditions set-up and brought to a successful completion (equilibrium solution reached). Interface properties were changed to the March 2004 conditions and analysis continued to a successful completion (equilibrium solution reached). Thus, results for the March 2004 conditions include the results of the May 2003 conditions. Results of these analyses are shown in Figs. 5 and 6. Figure 5 is for the May 2003 field conditions and shows: (a) progression of horizontal displacements at the three selected locations shown in Fig. 4a, (b) the spread of elastic, plastic-yield, and tension failure zones; and (c) the relative position of the slide mass. Figure 6 is a counterpart of Fig. 5 and is for the March 2004 field conditions. Table 4 shows the computed and field-observed displacements for the May 2003 and March 2004 conditions. Additional details of the static analysis are presented in Chugh and Stark 2005.

In brief, the computed and observed displacements at the corresponding locations for the May 2003 and March 2004 conditions are as follows: for the May 2003 field conditions—the computed horizontal and vertical displacement at the monitoring location 1 (head scarp) are 0.5 and 0.3 m, respectively while displacements observed in the field are: very limited horizontal movement and 1–2.5 m drop at the head-scarp; and for the March 2004 field conditions—the computed horizontal displacement at the monitoring location 3 (toe) is 36.1 m while field measurement is 23–30 m and the computed vertical displacement at the monitoring location 1 (head scarp) is 12.2 m while the field measurement is 7.5–9 m. Thus, comparisons between the computed and field observed displacements are good.

Seismic displacements

The seismic deformation analysis was applied to the static analysis model for the March 2004 conditions, Section under the sub-heading

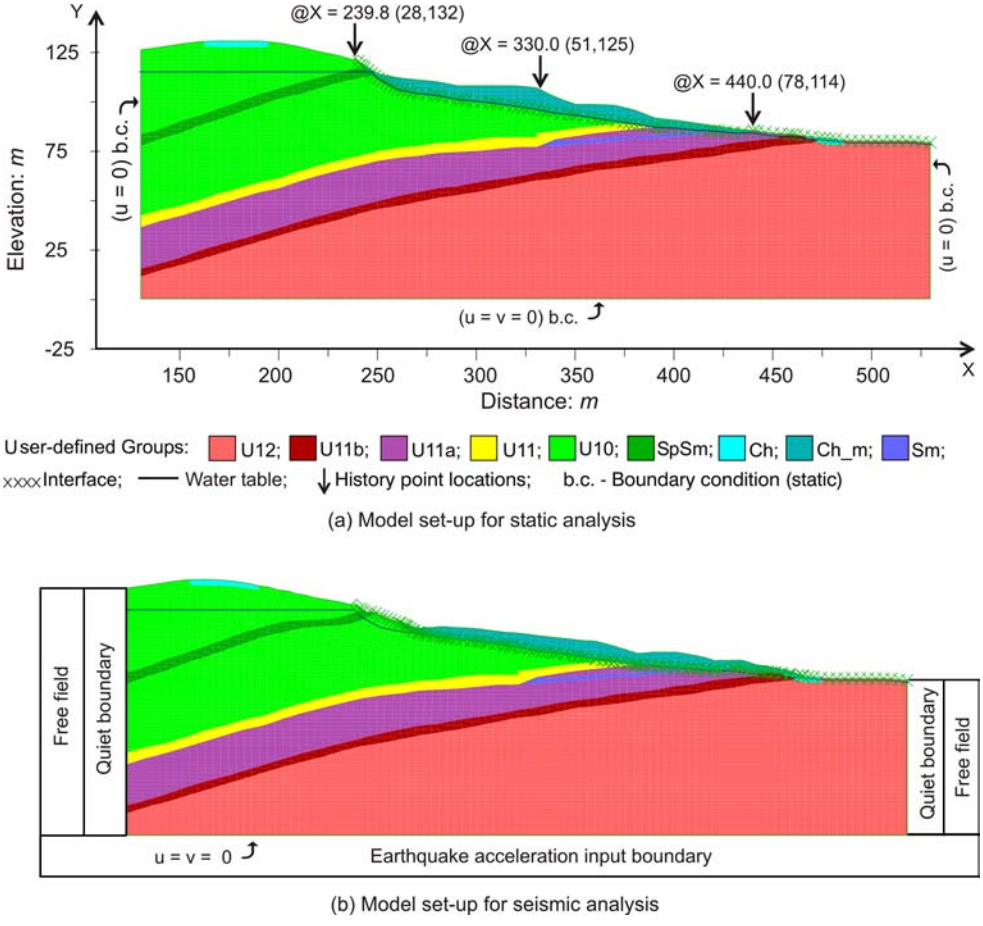

Fig. 4 FLAC model of the geologic cross section, Fig. 2c

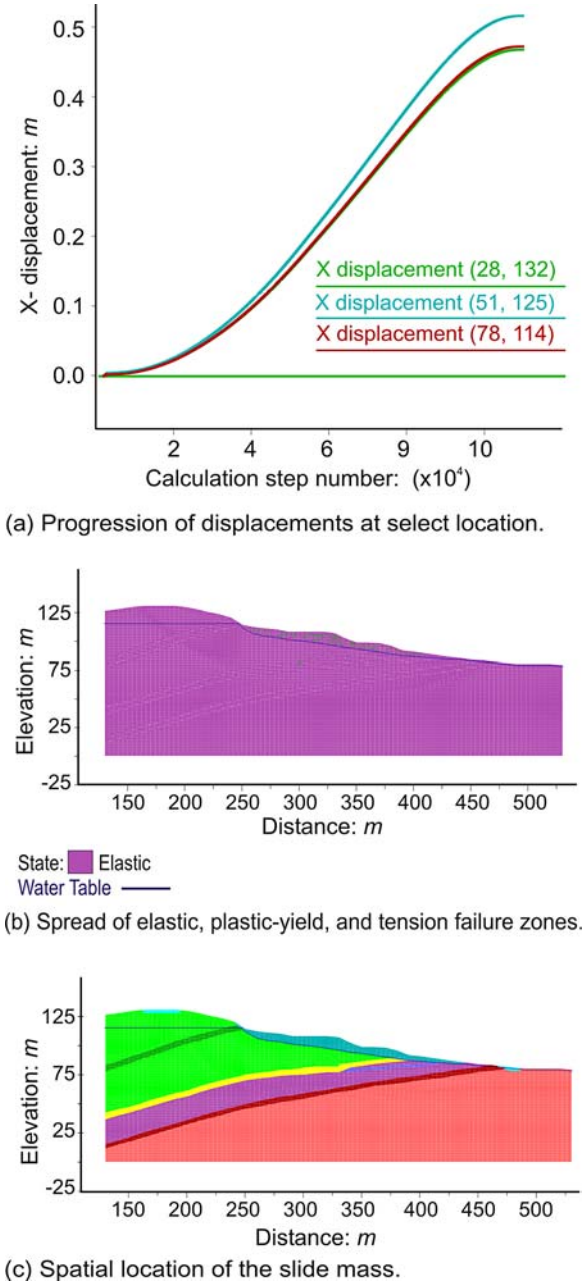

Fig. 5 Static analysis results using FLAC for the May 2003 conditions

'Static displacements'. The sequence of instructions followed for continuation of the static to seismic analysis conditions is (Fig. 4b):

(a) application of free-field boundaries to the sides of the model (which ensures transfer of static-equilibrium conditions to the free field);
(b) initializing velocities and displacements in the model from zero;
(c) initializing time histories of seismic acceleration, velocity, and displacement response at the selected locations in the model; and
(d) application of earthquake motion at the base of the model (Fig. 4b).

Thus, the dynamic displacements are in addition to the static displacement values determined in Section under the sub-heading 'Static displacements'. The earthquake duration is 40 s (Fig. 3) and at the end of 40 s, the applied acceleration and velocity to the model are set to zero, and the dynamic analysis continued to 60 s to observe the model response for 20 s past the end of the earthquake motion (free vibrations). Rayleigh damping of 5% of critical damping operating at a central frequency of 2 Hz was used in all dynamic analyses.

Variations in displacement, velocity, and acceleration with respect to time (history) at the updated select locations shown in Fig. 4a were recorded at dynamic times of 1, 10, 20, 30, 40, 50, and 60 s, and the corresponding model state was saved. The computed acceleration, velocity, and displacement histories at 60 s are shown in Fig. 7a, b, and c, respectively; they are all inclusive for the model subjected to

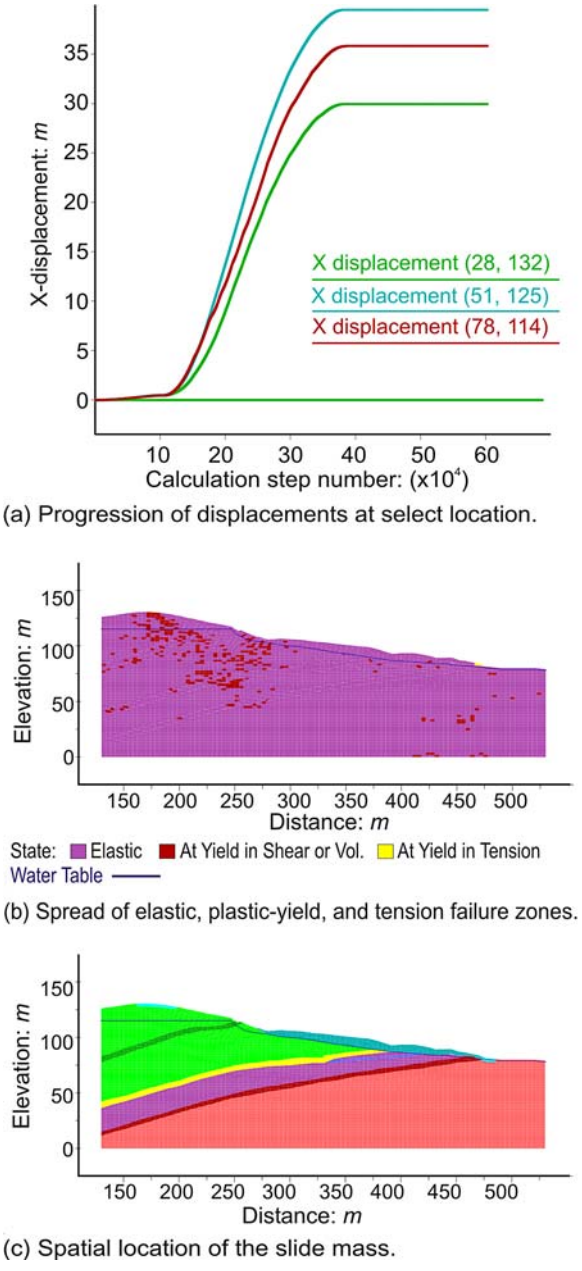

Fig. 6 Static analysis results using FLAC for the March 2004 conditions

Table 4 Comparison of displacement results with the field data (Table 1)

Condition	May 2003		March 2004		Seismic (future)	
	Downslope movement at head-scarp (m)	Vertical drop at head scarp (m)	Downslope movement at toe (m)	Vertical drop at head scarp (m)	Downslope movement at toe (m)	
Field measurements	Very limited	1–2.5	23–30	7.5–9	N/A	
FLAC results	*x*-displacement (m)	*y*-displacement (m)	*x*-displacement (m)	*y*-displacement (m)	*x*-displacement (m)	*y*-displacement (m)
	0.5	−0.3	36.1	−12.2	2.2	0.2
DISP results	N/A	N/A	N/A	N/A	2.0 m for yield acceleration of 0.005 g	

N/A not applicable; negative *y* direction in the FLAC model corresponds to drop in elevation

Table 5 Seismic displacement results for the reversed sign of accelerations in the earthquake motion shown in Fig. 3

Condition	Seismic (future)	
	x-displacement at toe (m)	*y*-displacement at toe (m)
FLAC results	2.4	0.2
DISP results	5.0 m in the downslope direction for yield acceleration of 0.005 g	

the seismic input. The stair-step nature of the displacement history and the cyclic nature of the velocity plots (except for the negative velocity parts) illustrate the deformations and velocities implied in the Newmark procedure for seismically-induced slope deformations. The calcualted permanent horizontal displacement at monitoring location 3 (toe) due to the seismic input of Fig. 3 is 2.2 m (Fig. 7c and Table 4). The static horizontal displacement is 36.1 m. Therefore, for Qls-18 landslide, the computed total permanent displacement at monitoring location 3 (toe) is 38.3 m.

Figure 8 shows the spread of elastic, plastic-yield, and tension failure zones at 1, 10, 20, 30, 40, 50, and 60 s. It is interesting to note the changes in response of the material model during and following the application of earthquake motion.

DISP model

Figure 9 presents a schematic description of the Newmark Sliding Block procedure for seismically-induced slope deformations (Newmark 1965; Chugh 1982, 1995). The base angle α for the March 2004 configuration of the slide mass is estimated to be about 5.67°; the base angle α_1 for the next 10 m distance is estimated to be about 5.71°. For the March 2004 slope configuration, the static FoS (using FLAC) is 1.01 but the failure surface is different from the one along which displacements are being assessed. Defining the interface as the failure surface (along which displacements are being assessed) in the limit-equilibrium based procedure implemented in the computer program SSTAB2 (Chugh 1992), the static FoS (for the March 2004 configuration of the slide mass) is 0.92 with an interslice force inclination of 6.5°. Therefore, a low value of 0.005 g was assumed (without calculation) for the yield acceleration of the slide mass. The earthquake motion of Fig. 3 was used without propagating it through the soil mass. For these conditions, the dynamic displacement is calculated to be about 2 m in the downslope direction. The acceleration, velocity, and displacement history results from DISP are shown in Fig. 10. A permanent downslope displacement of 2 m by the Newmark procedure (DISP) is in excellent agreement with the resultant seismic displacement of about 2.21 m estimated using the continuum-mechanics-based procedure (FLAC), see Table 4.

Sensitivity analyses

Reversing the sign of acceleration values in the earthquake data

The Loma Prieta earthquake motion (Fig. 3) has a peak acceleration of about 0.24 g positive and about 0.30 g negative. The dynamic displacements, using FLAC and DISP, were also made using a time-acceleration record with reversed polarity. Results of these calculations are shown in Fig. 11 and Table 5. Reversing the sign of acceleration values in the earthquake data in the continuum approach did not result in significant change in the computed displacements at the toe of the landslide (FLAC results for seismically induced *x*-displacement of 2.4 m vs. 2.2 m in Tables 5 and 4, respectively). However, reversing the sign of acceleration values in the earthquake data in the Newmark procedure resulted in significant increase in the computed downslope displacements (DISP results for seismically induced downslope movement of 5.0 m vs. 2.0 m in Tables 5 and 4, respectively). The precise reason for this relatively large difference in computed displacements by the two procedures (FLAC and DISP) is not clear at this time. However, the objective lesson in this sensitivity element is that a polarity change in a non-simulated seismic motion should be considered in analysis of numerical models by repeating the analyses for different combinations of polarity change in the input motion. Thus, for the Qls-18 landslide, the computed total permanent *x*-displacement at the toe could be upto about 41 m (36 m static plus 5 m seismic).

Effect of variation in yield acceleration in Newmark approach

The dynamic displacement calculations for the DISP model were also made by varying yield acceleration values from 0.001 g to 0.01 g in increments of 0.001 g. Results of these calculations for the earthquake motion shown in Fig. 3 and also for the reversed sign of accelerations are shown in Fig. 12. Variations in dynamic displacements of a slide mass using the Newmark approach are rightfully sensitive to the yield acceleration which relates to the static stability (FoS)—the

Table 6 Static and seismic displacement results for the $G = 1.0 \times 10^6$ kPa and $K = 1.5 \times 10^6$ kPa

Condition	May 2003		March 2004		Seismic (future)	
	x-displacement (head scarp) (m)	*y*-displacement (head scarp) (m)	*x*-displacement (toe) (m)	*y*-displacement (head scarp) (m)	*x*-displacement (toe) (m)	*y*-displacement (toe) (m)
FLAC results	0.4	−0.2	46.0	−13.1	4.2	0.4

Negative *y* direction in the FLAC model corresponds to drop in elevation

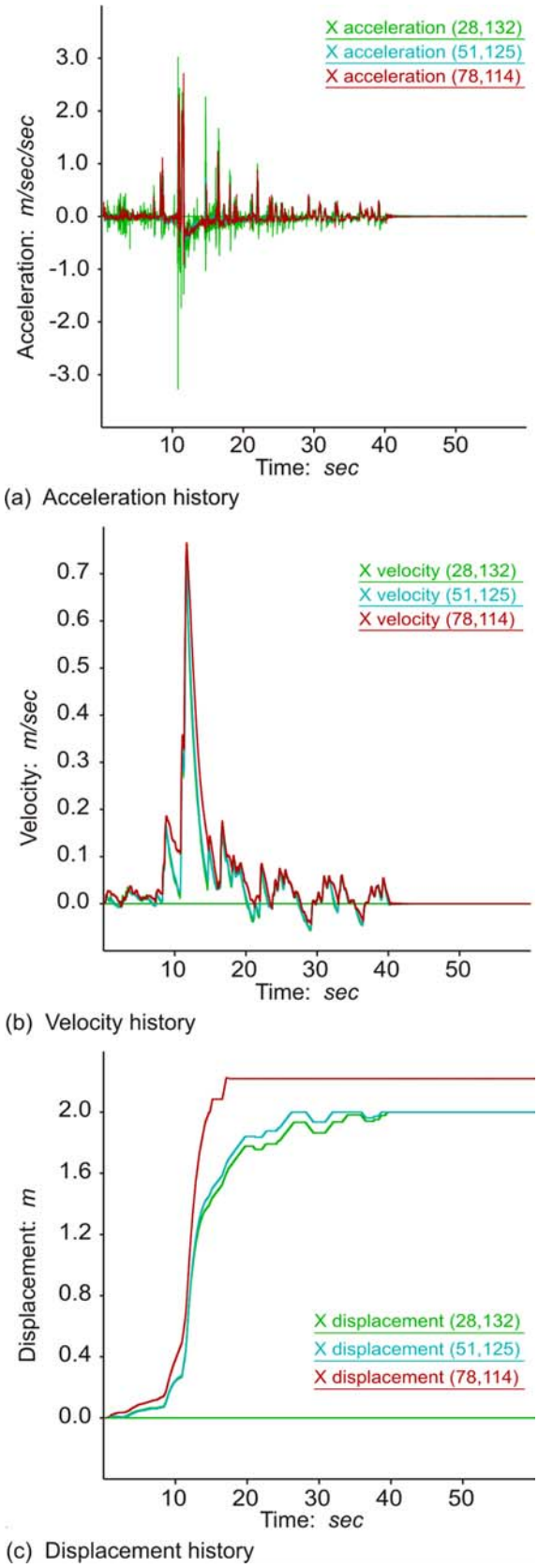

Fig. 7 Seismic analysis results for the FLAC model at the end of 60 s for the Loma Prieta earthquake

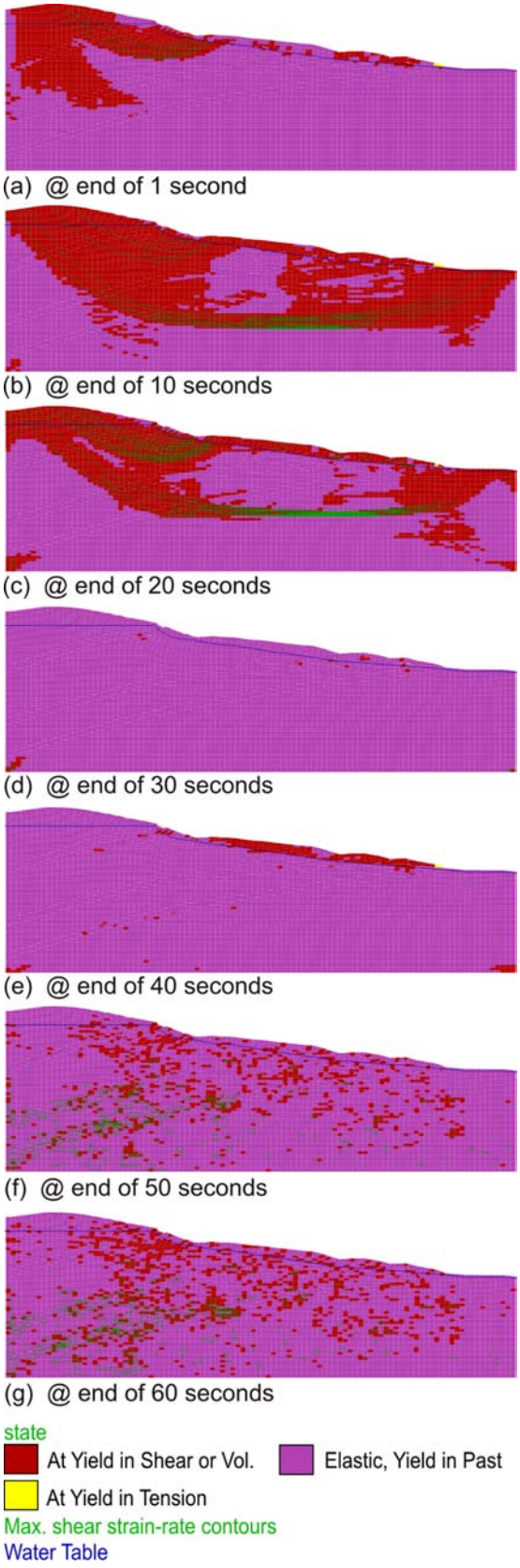

Fig. 8 Spread of elastic, plastic-yield, failed-in-tension zones, and shear strain rate contours during the earthquake

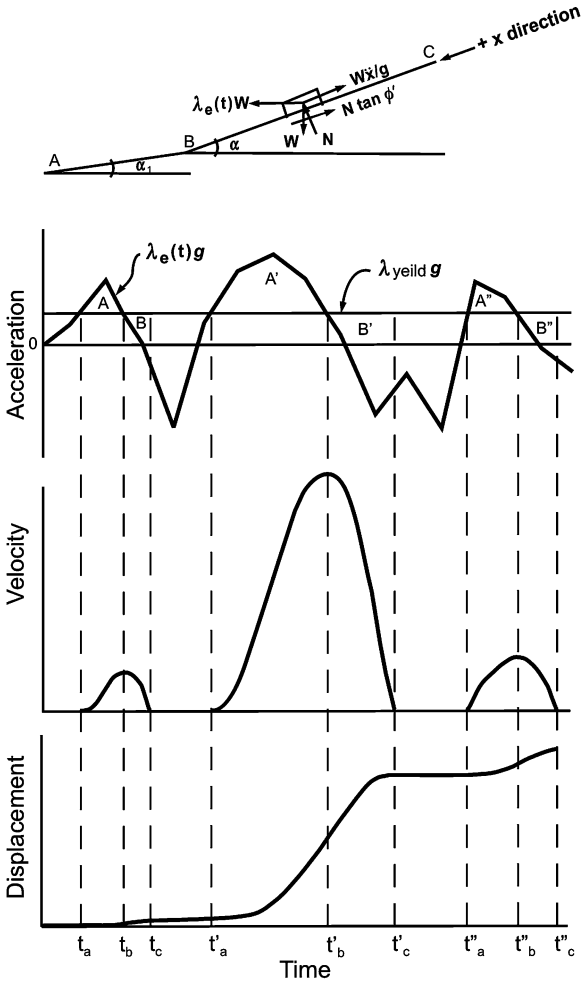

Equations of motion along the slide planes (Chugh 1982)

$$\left|\frac{d^2x}{dt^2}\right| = \frac{\cos(\alpha - \phi')}{\cos\,\phi'}\,(\lambda_e - \lambda_{yield})\,g$$

along BC

$$\left|\frac{d^2x}{dt^2}\right| = \frac{\cos(\alpha - \phi')}{\cos(\alpha - \alpha_1 - \phi')}\,(\lambda_e - \lambda_{yield})\,g$$

from BC to BA

Fig. 9 DISP model for seismically-induced displacements using Newmark procedure

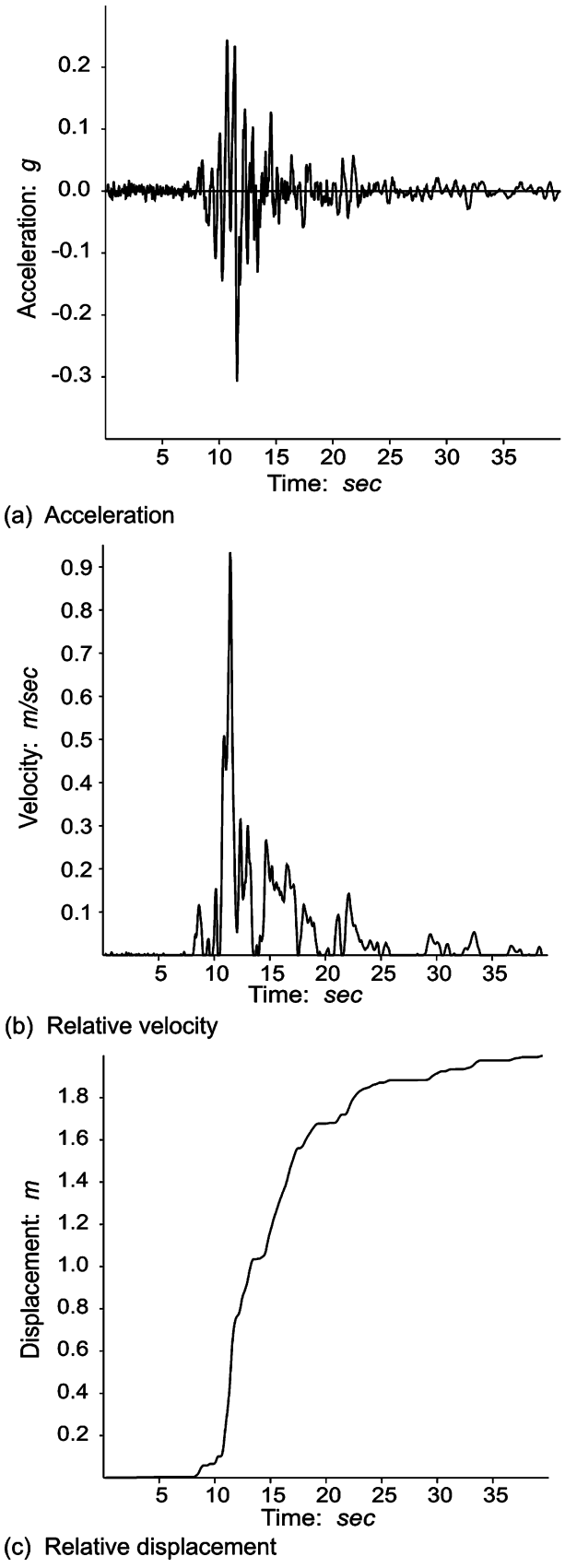

Fig. 10 Seismically-induced displacement results using DISP

only question is of the order of sensitivity (Chugh 1995). It is understood that a marginally stable earth-mass (low FoS and hence low yield-acceleration) shall experience larger displacements during an earthquake than if it had high static stability. Other factors affecting the magnitude of dynamic displacements of an earth-mass include: (a) the geometry of the riding surface, and (b) the kinetic energy of the slide mass.

Elastic constants

The shear modulus, G, and the bulk modulus, K, were assigned values of 1.0×10^7 kPa and 1.5×10^7 kPa, respectively in the results reported in Tables 4 and 5, and in Figs. 5–8. For $G = 1.0 \times 10^4$ kPa and $K = 1.5 \times 10^4$ kPa, the FLAC model runs into numerical problems due to excessive changes in geometry. For $G = 1.0 \times 10^6$ kPa and $K = 1.5 \times 10^6$ kPa, the static- and seismic- displacement results are shown

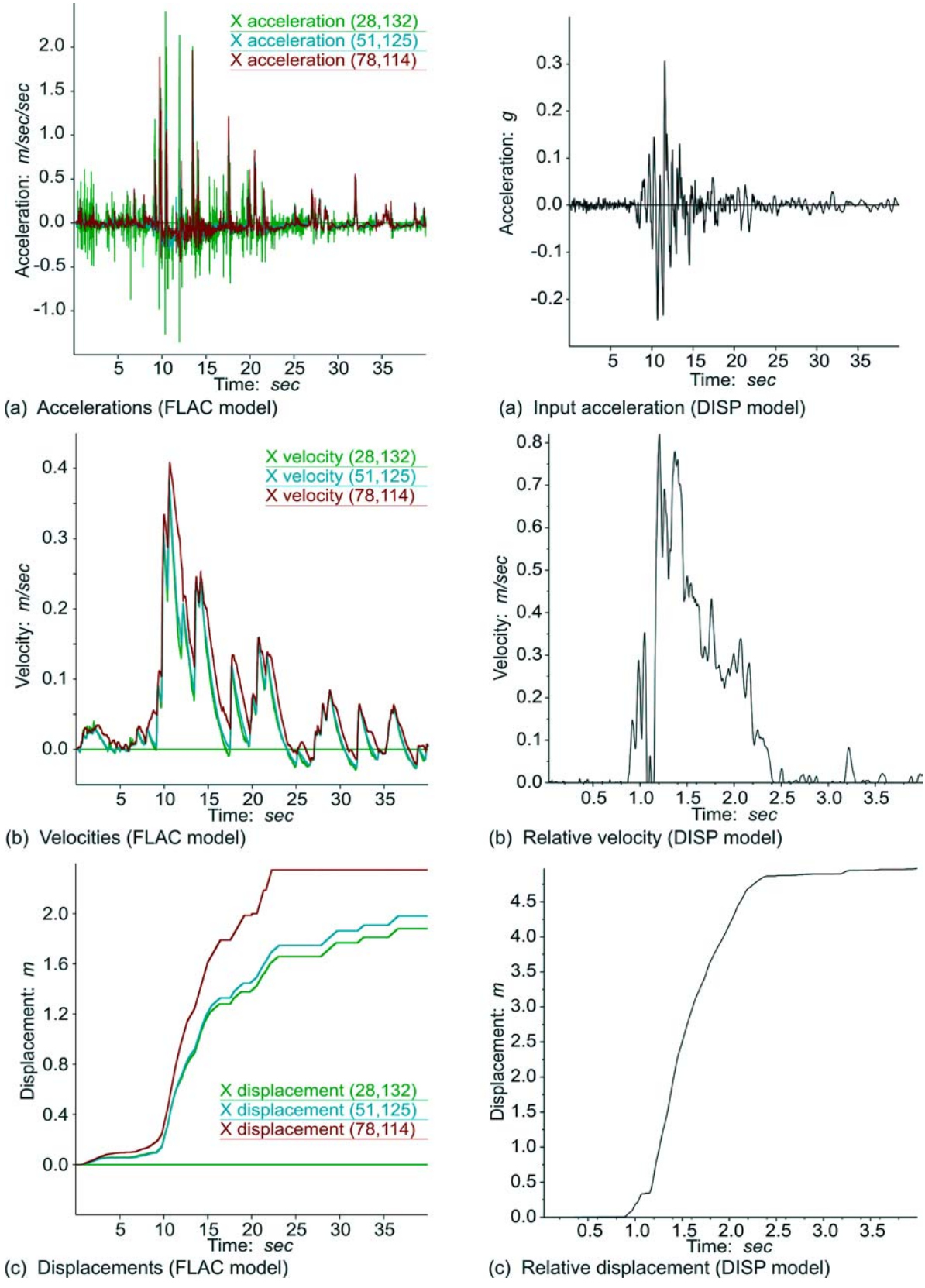

Fig. 11 Seismic analysis results of interest for reversed polarity of input motion of Fig. 3: FLAC and DISP models

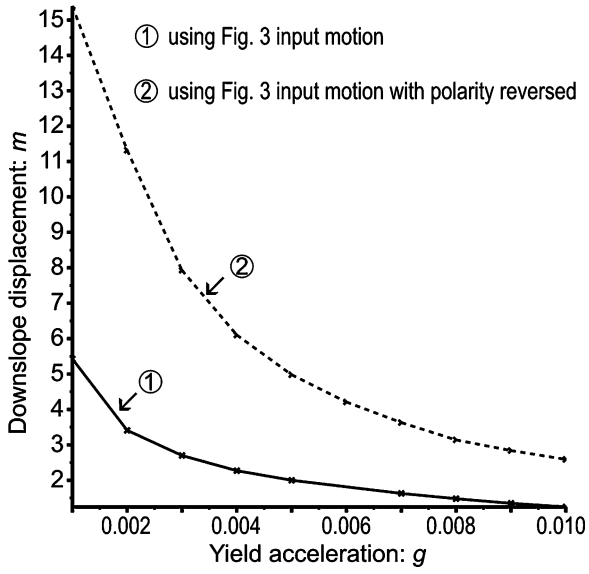

Fig. 12 Sensitivity of dynamic displacements to variations in yield acceleration: DISP model

in Table 6. There is a noticeable increase in static displacements for the March 2004 conditions (46.0 m in Table 6 vs. 36.1 m in Table 4) and seismic displacements also increase (4.2 m in Table 6 vs. 2.2 m in Table 4) due to the lowering of the G and K values. However, for the March 2004 conditions, the computed values of static displacements (using $G = 1.0 \times 10^6$ kPa and $K = 1.5 \times 10^6$ kPa) differ significantly from the field measured values shown in Table 1 (46.0 m in Table 6 vs. 23–30 m in Table 1). Therefore, the use of $G = 1.0 \times 10^6$ kPa and $K = 1.5 \times 10^6$ kPa is not considered appropriate for the Qls-18 landslide.

General comments

(a) Seismic analysis of field problems using continuum-mechanics based procedures with Rayleigh (stiffness and mass proportional) damping is generally very time consuming – using FLAC, each seismic analysis of the Qls-18 landslide reported in this paper took well over 240 h on a well equipped modern personal computer. All calculations were performed using single-precision arithmetic (use of double-precision arithmetic was not successful in bringing the FLAC model to a stable state for the March 2004 conditions).

(b) FLAC in large-strain mode updates the coordinates of the grid at each calculation step, but the constitutive formulation is that of small strains.

(c) Seismic displacement calculations using the Newmark procedure are very efficient—using DISP, each seismic displacement calculation of the Qls-18 landslide reported in this paper took well under 1 min on the same personal computer as in (a).

(d) Analytical and numerical details of the static, dynamic, and interface logic used in analyses reported in this paper are given in FLAC manuals (Itasca Consulting Group 2000). Details of the limit-equilibrium procedure used for static FoS results reported in this paper are given in the SSTAB2 manual (Chugh 1992). Details of the Newmark procedure used in this paper are given in the DISP manual (Chugh 1980). These details are not included here to conserve space.

Conclusions

(a) The computed permanent displacements of Qls-18 landslide using the proposed procedure in a continuum-mechanics based procedure FLAC are in good agreement with the May 2003 and March 2004 field data which pertain to the onset and a stable configuration of the landslide, respectively. Seismically induced permanent displacements of Qls-18 landslide using the proposed procedure in FLAC are in fair agreement with the Newmark's rigid block procedure implemented in DISP.

(b) Safety of the people and property (presently located within about 50 m from the toe of the slide) against the hazards of the landslide can not be assured because there could occur additional movements of the slide mass due to possible further reductions in shear strengths of materials due to weathering; increase in pore water pressure due to rise in ground-water level in the hills; and infiltration from surface run-off from rain storms. Seismic concerns at this site are even larger. There exists a possibility that the slide mass may turn into a mud flow during a heavy rain storm or a strong seismic event. Therefore, for safety of people and property, it is better to err on the side of safety.

(c) Static deformation analyses can be performed effectively and efficiently using the continuum approach. It is instructive and informative to perform displacement analysis following a slope stability analysis using residual strength values along the interface representing the most vulnerable shear surface.

(d) Dynamic deformation analysis using the continuum approach is very time-consuming and should be performed when refinements to dynamic deformation results using the Newmark procedure are considered necessary. However, additional comparisons between the results of these two procedures on field problems are warranted to gain confidence in this recommendation.

Acknowledgements

The authors would like to express their sincere thanks to Dr. Robert L. Schuster for his constructive comments and suggestions on the initial draft of the paper.

References

Chugh AK (1980) User information manual: Dynamic slope stability displacement program DISP. U.S. Bureau of Reclamation, Engineering and Research Center, Denver, Colorado

Chugh AK (1982) Slope stability analysis for earthquakes. Int J Num Anal Methods Geomech 6:307–322

Chugh AK (1992) User information manual: Slope stability analysis program SSTAB2. U.S. Bureau of Reclamation, Engineering and Research Center, Denver, Colorado

Chugh AK (1995) Dynamic displacement analysis of embankment dams. Géotechnique 45(2):295–299

Chugh AK, Stark TD (2005) Displacement analysis of a landslide. In: 11th international conference and field trip on landslides, Norway, 1–10 September 2005

Itasca Consulting Group (2000) FLAC—Fast Lagrangian Analysis of Continua. Itasca Consulting Group, Minneapolis, Minnesota

Newmark NM (1965) Effects of earthquakes on dams and embankments. Geotechnique 15(2):139–159

U.S. Bureau of Reclamation (2004) Internal reports. Denver, Colorado

A. K. Chugh (✉)
U.S. Bureau of Reclamation, Denver,
Colorado 80225, USA
e-mail: Achugh@do.usbr.gov
Tel.: +303-445-3026
Fax: +303-445-6432

T. D. Stark
University of Illinois, Urbana,
Illinois 61801, USA